Supplement of Atmos. Chem. Phys., 23, 15589–15607, 2023
https://doi.org/10.5194/acp-23-15589-2023-supplement

Atmospheric Chemistry and Physics
Open Access
EGU

Supplement of

Drivers controlling black carbon temporal variability in the lower troposphere of the European Arctic

Stefania Gilardoni et al.

Correspondence to: Stefania Gilardoni (stefania.gilardoni@cnr.it) and Radovan Krejci (radovan.krejci@aces.su.se)

Supplement

S1. Selection of the Mass Absorption Cross section

MAC of freshly emitted BC particles is centered around 7.5 m^2g^{-1} at 550 nm (Bond and Bergstrom, 2006). Far from emission sources, BC particles aged by atmospheric processing and characterized by non-absorbing coating show higher MAC values (Cross et al., 2010; Lack et al., 2012). Such absorption enhancement varies with particle fractal dimension, coating, and internal mixing geometry (Knox et al., 2009; Cappa et al., 2012). For example, Zanatta et al. (2018) estimated an 240 enhancement of BC absorption in the Arctic equal to 54%(Zanatta et al., 2018). In addition, BC MAC reported in literature depends on the techniques employed for the determination of aerosol light absorption and BC mass concentration. BC MAC reported by previous studies based on aethalometer measurements over two years in southern Scandinavia ranged between 7.6 and 9.1 m^2g^{-1} (Zanatta et al., 2016), which is equivalent to 8.8 - 10.5 m^2g^{-1} at 550 nm. Combining aethalometer and refractory BC measurements, Zanatta et al. derived a MAC of 9.8 m^2g^{-1} at 550 nm in Svalbard in spring (Zanatta et al., 2018). MAC of BC at Nunavut (Alert , 82.5N) was determined using aethalometer aerosol absorption data collected during almost three years and averaged between 5 and 9 m^2g^{-1} at 550 nm, depending on the season (Sharma et al., 2017). Ohata et al. (2021) reported BC MAC at 550 nm for five different Arctic sites over 10 years and using aerosol absorption measurements performed with different filter-based photometers. The observed MAC ranged between 10.8 and 15.1 m^2g^{-1} (Ohata et al., 2021). In the present study we derive eBC concentration using the MAC value reported by Ohata et al. (2021) and calculated for MAAP measurements performed in the Svalbard archipelago. Such value corresponds to 10.2 m^2g^{-1} at 660 nm, assuming an absorption angstrom exponent of 1. We decided to use the MAC derived from MAAP rather than PSAP measurements, because PSAP measurements at GAL were comparable to MAAP data (section 3.1), while PSAP correction algorithm adopted by Ohata et al. (2021) differs from the one employed in this study.

Table S1. MAC values reported from previous studies in the Arctic region.

MAC at 550nm	Notes	Reference
7.5 m^2g^{-1}	Freshly emitted BC	Bond and Bengstrom, 2006
8.8 – 10.5 m^2g^{-1}	Arctic	Zanatta et al. 2016
9.8 m^2g^{-1}	Svalbard (spring)	Zanatta et al. 2018
5 – 9 m^2g^{-1}	Alert (3 year data)	Sharma et al., 2017
10.8 – 15.1 m^2g^{-1}	Arctic	Ohata et al. 2021

S2. Back-trajectory analysis

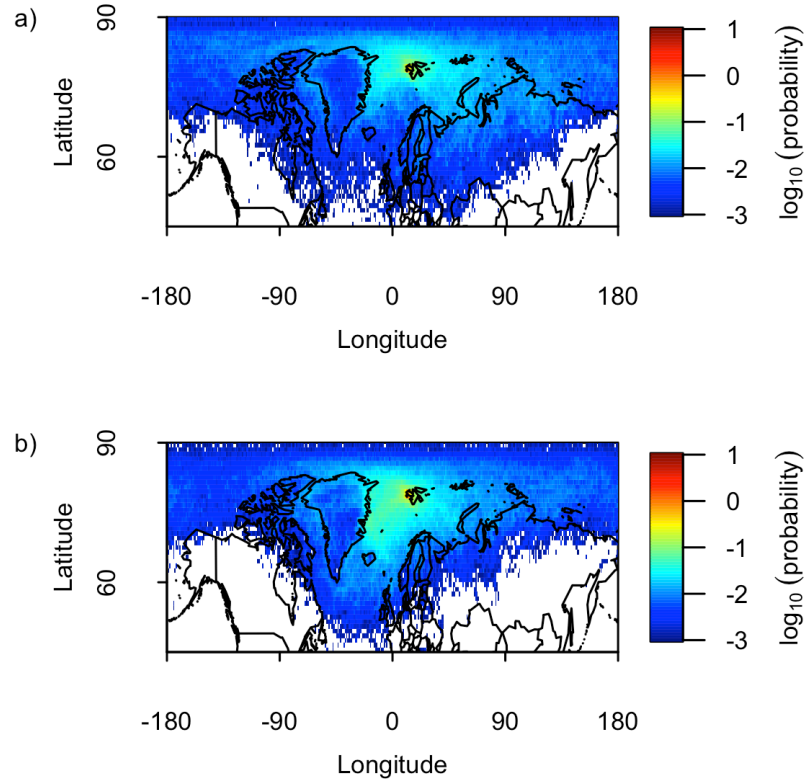

Figure S1. Probability residence time map of the cold (panel a) and warm (panel b) season from 7-day LAGRANTO back trajectories.

S3. BC emissions

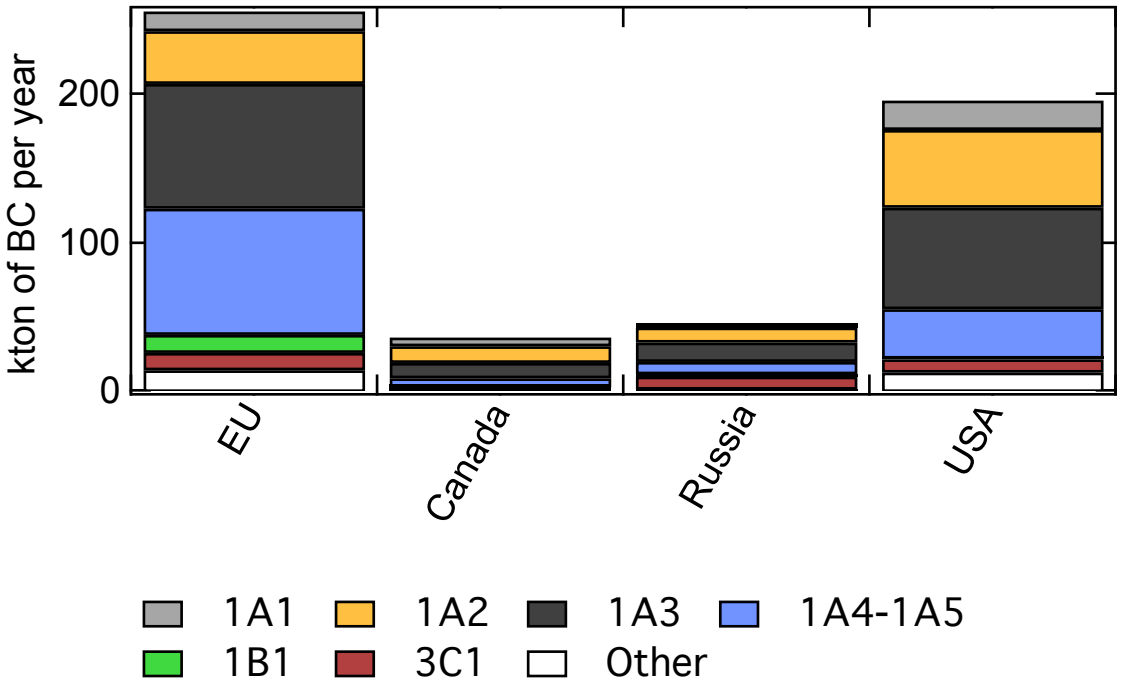

Figure S2. Share of 2018 BC emissions from Europe (EU), Canada, Russia, and United States of America (USA), corresponding to power industry and oil refinery and transformation industry (1A1), combustion for manufacturing (1A2), transportation (1A3), energy for buildings (1A4-1A5), fuel exploitation (1B1), agricultural waste burning (3C1), and other sectors. BC emissions are derived from EDGARv6.1 emission database (https://edgar.jrc.ec.europa.eu).

S4. Analysis of drivers controlling eBC variability

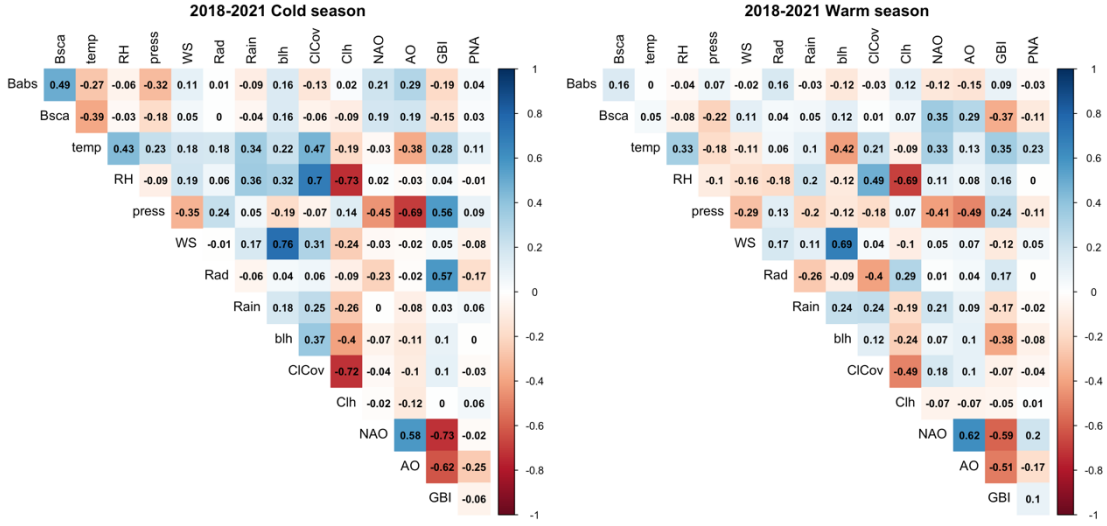

Figure S3. Pearson correlation matrix of eBC concentration, meteorological variables, and general circulation indexes for the cold (November – April) and the warm period (May -October).

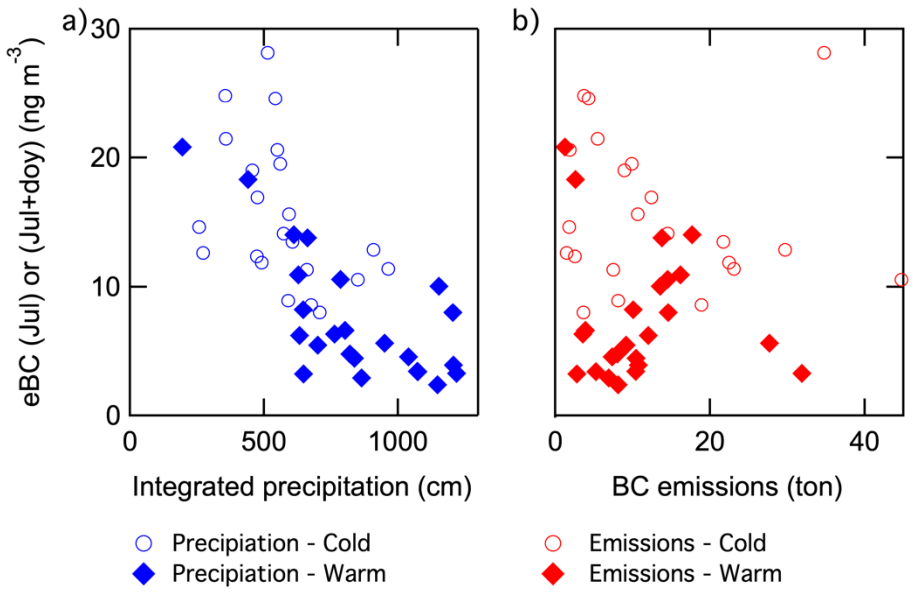

Figure S4. eBC monthly averages modeled by GAM, based on Julian day in the cold season and Julian day and day of the year in the warm season, as a function of precipitation (a) and BC emissions (b), integrated along back-trajectories.

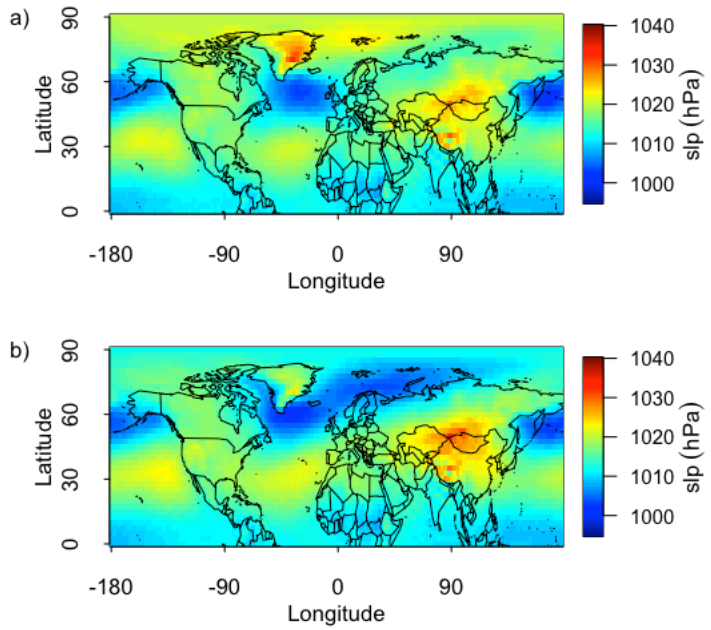

Figure S5. Average sea level pressure maps when atmospheric pressure at GAL was higher than 1010 hPa in the cold season (panel a) and during the entire cold season (panel b).

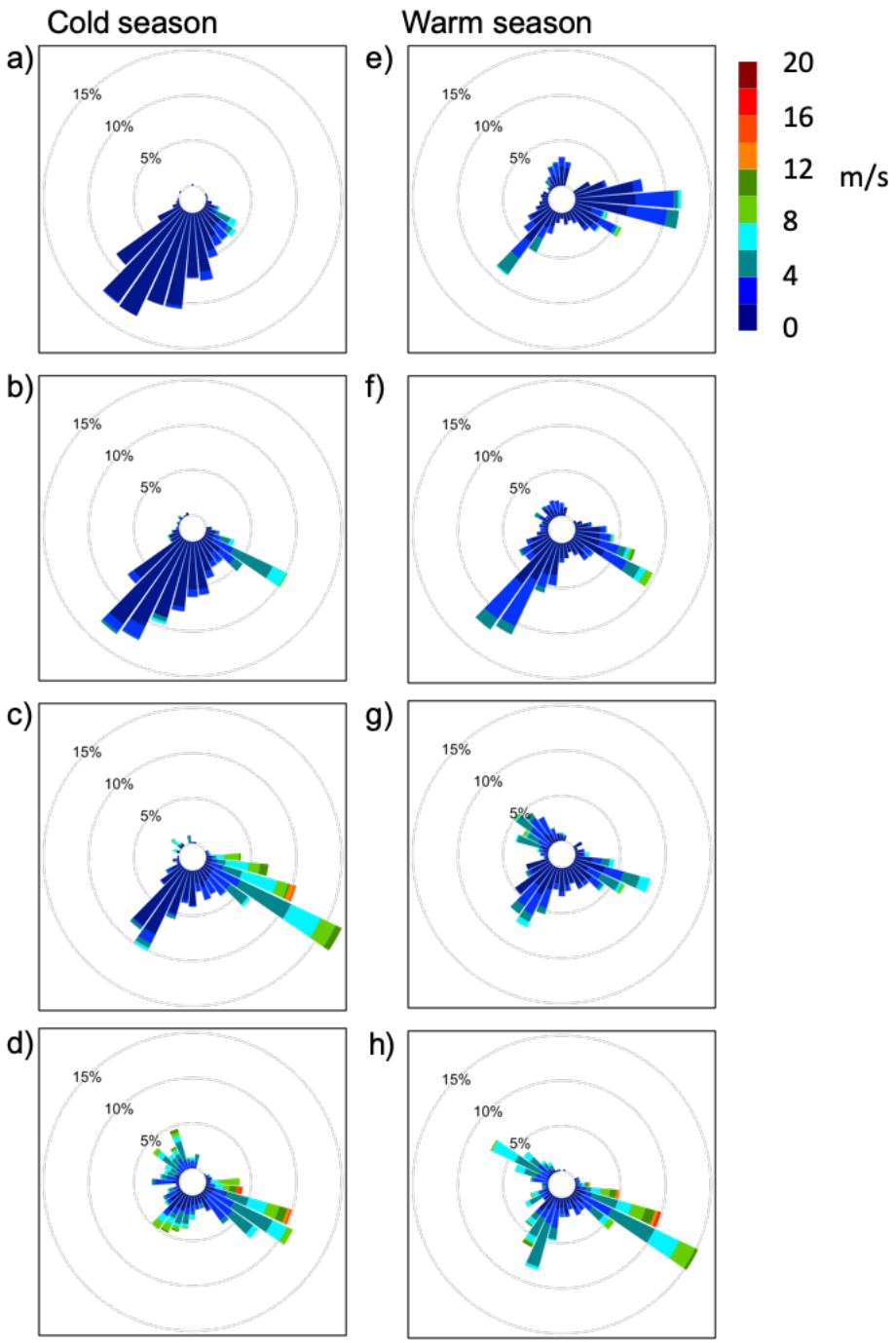

Figure S6. Wind roses describing main wind pattern at GAL during the cold (a-d) and the warm season(e-h) when blh was below 100 m (a and e), between 100 and 200 m (b and f), between 200 and 400 m (c and g), and between 400 and 600 m (d and h).

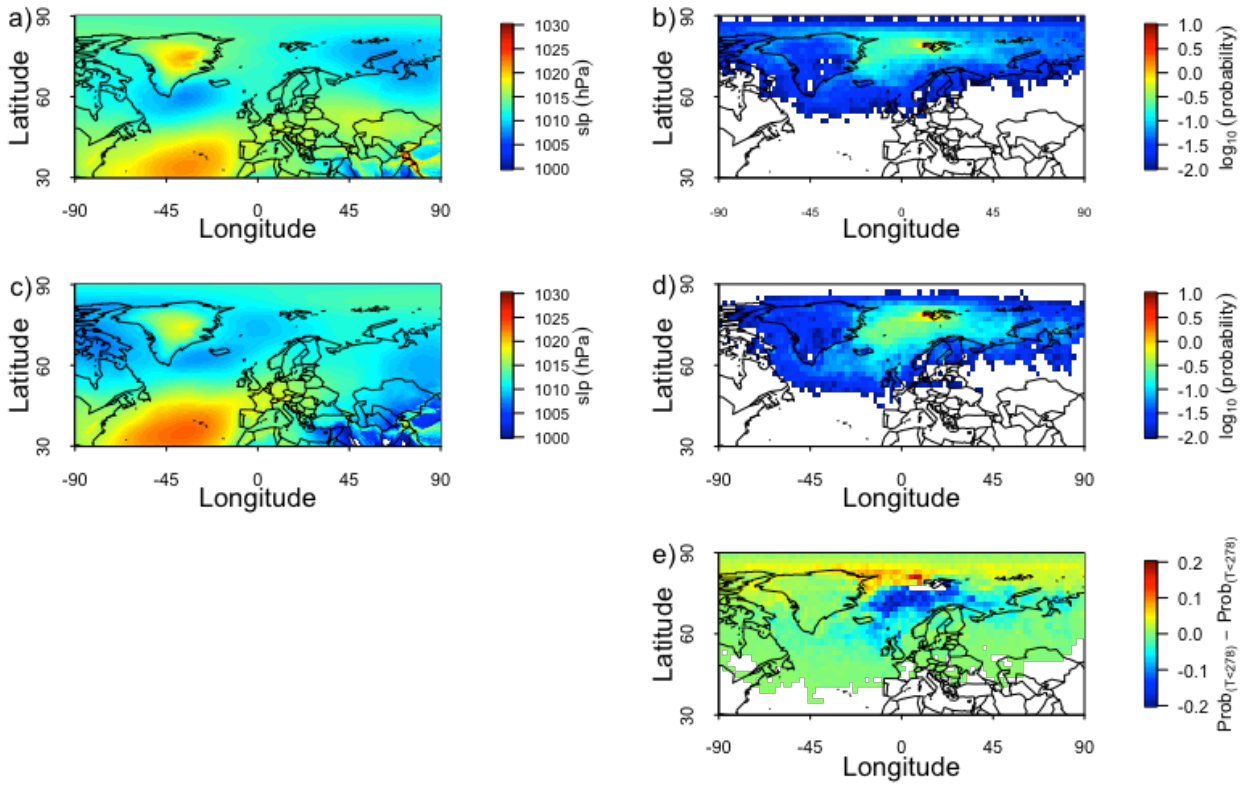

Figure S7. Average sea level pressure maps and residence time probability maps when the temperature at GAL was lower (panel a and c) and higher (panel b and d) than 278 K during the warm season. Residence time probability maps are based on 7-day back-trajectories. The threshold of 278 K was defined based on the temperature impact on eBC concentration reported in Fig. 7c. Panel e shows the probability difference map between colder and warmer days (panel b – panel d).

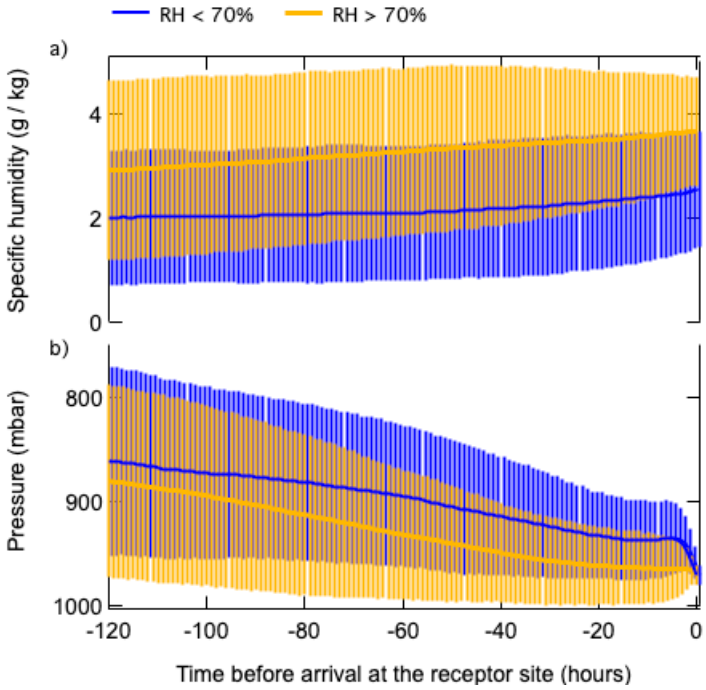

Figure S8. Change of specific humidity (panel a) and pressure (panel b) along back-trajectories, for air masses arriving at GAL when RH was higher (orange) and lower (blue) than 70%. Continuous lines indicate mean values, while vertical lines correspond to standard deviation.

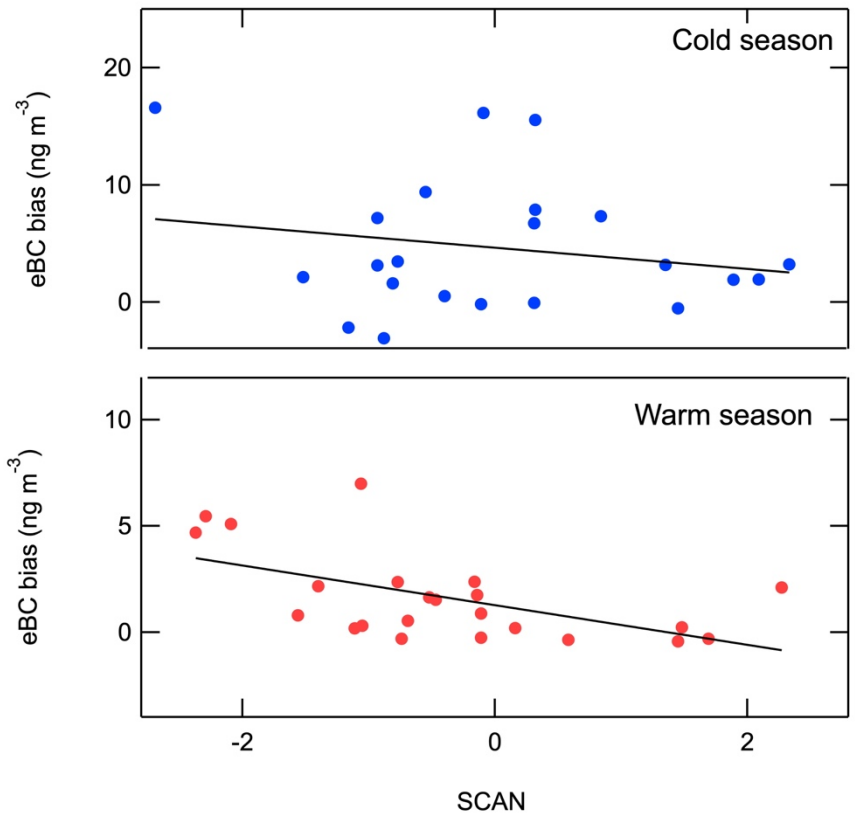

Figure S9. Relationship between GAM monthly biases and SCAN index.

References

Bond, T. C. and Bergstrom, R. W.: Light Absorption by Carbonaceous Particles: An Investigative Review, Aerosol Science and Technology, 40, 27-67, 10.1080/02786820500421521, 2006.

Cappa, C., Onasch, T., Massoli, P., Worsnop, D., Bates, T., Cross, E., Davidovits, P., Hakala, J., Hayden, K., Jobson, B., Kolesar, K., Lack, D., Lerner, B., Li, S., Mellon, D., Nuaaman, I., Olfert, J., Petaja, T., Quinn, P., Song, C., Subramanian, R., Williams, E., and Zaveri, R.: Radiative Absorption Enhancements Due to the Mixing State of Atmospheric Black Carbon, Science, 337, 1078-1081, 10.1126/science.1223447, 2012.

Cross, E. S., Onasch, T. B., Ahern, A., Wrobel, W., Slowik, J. G., Olfert, J., Lack, D. A., Massoli, P., Cappa, C. D., Schwarz, J. P., Spackman, J. R., Fahey, D. W., Sedlacek, A., Trimborn, A., Jayne, J. T., Freedman, A., Williams, L. R., Ng, N. L., Mazzoleni, C., Dubey, M., Brem, B., Kok, G., Subramanian, R., Freitag, S., Clarke, A., Thornhill, D., Marr, L. C., Kolb, C. E., Worsnop, D. R., and Davidovits, P.: Soot Particle Studies—Instrument Inter-Comparison—Project Overview, Aerosol Science and Technology, 44, 592-611, 10.1080/02786826.2010.482113, 2010.

Knox, A., Evans, G. J., Brook, J. R., Yao, X., Jeong, C. H., Godri, K. J., Sabaliauskas, K., and Slowik, J. G.: Mass Absorption Cross-Section of Ambient Black Carbon Aerosol in Relation to Chemical Age, Aerosol Science and Technology, 43, 522-532, 10.1080/02786820902777207, 2009.

Lack, D. A., Langridge, J. M., Bahreini, R., Cappa, C. D., Middlebrook, A. M., and Schwarz, J. P.: Brown carbon and internal mixing in biomass burning particles, Proceedings of the National Academy of Sciences, 109, 14802-14807, doi:10.1073/pnas.1206575109 %U https://www.pnas.org/doi/abs/10.1073/pnas.1206575109, 2012.

Ohata, S., Mori, T., Kondo, Y., Sharma, S., Hyvärinen, A., Andrews, E., Tunved, P., Asmi, E., Backman, J., Servomaa, H., Veber, D., Eleftheriadis, K., Vratolis, S., Krejci, R., Zieger, P., Koike, M., Kanaya, Y., Yoshida, A., Moteki, N., Zhao, Y., Tobo, Y., Matsushita, J., and Oshima, N.: Estimates of mass absorption cross sections of black carbon for filter-based absorption photometers in the Arctic, Atmos. Meas. Tech., 14, 6723-6748, 10.5194/amt-14-6723-2021, 2021.

Sharma, S., Leaitch, W. R., Huang, L., Veber, D., Kolonjari, F., Zhang, W., Hanna, S. J., Bertram, A. K., and Ogren, J. A.: An evaluation of three methods for measuring black carbon in Alert, Canada, Atmos. Chem. Phys., 17, 15225-15243, 10.5194/acp-17-15225-2017, 2017.

Zanatta, M., Laj, P., Gysel, M., Baltensperger, U., Vratolis, S., Eleftheriadis, K., Kondo, Y., Dubuisson, P., Winiarek, V., Kazadzis, S., Tunved, P., and Jacobi, H.: Effects of mixing state on optical and radiative properties of black carbon in the European Arctic, Atmospheric Chemistry and Physics, 18, 14037-14057, 10.5194/acp-18-14037-2018, 2018.

Zanatta, M., Gysel, M., Bukowiecki, N., Müller, T., Weingartner, E., Areskoug, H., Fiebig, M., Yttri, K. E., Mihalopoulos, N., Kouvarakis, G., Beddows, D., Harrison, R. M., Cavalli, F., Putaud, J. P., Spindler, G., Wiedensohler, A., Alastuey, A., Pandolfi, M., Sellegri, K., Swietlicki, E., Jaffrezo, J. L., Baltensperger, U., and Laj, P.: A European aerosol phenomenology-5: Climatology of black carbon optical properties at 9 regional background sites across Europe, Atmospheric Environment, 145, 346-364, https://doi.org/10.1016/j.atmosenv.2016.09.035, 2016.